SPECIAL

Roman Bogacz · Włodzimierz Kurnik

On some rotor-dynamical phenomena of high-speed trains

Abstract The paper is devoted to radial and out-of-plane vibration of railway wheels and to wheelset stability as key elements affecting high-speed vehicle dynamics, noise emission, and safety. In the present study, railway wheel tire is treated as a curved beam with various beam models, and the wheel plates are modeled as Winkler's elastic foundation. New results are presented concerning the influence of the residual stresses on the corrugation and poligonalization of wheels as well as wave propagation in the wheel tire.

Keywords Elastic wheel · Wheel–rail interaction · Traveling waves · Wheel poligonalization · Corrugation

1 Introduction

The cost-efficiency, maintenance, comfort and safety of railway operation depend strongly on the quality of the wheelset–track interaction. The wheel rim movement has a great impact on the above-mentioned subjects; thus, the study of wheel rim behavior is of very great importance. Design of rotating elements of modern high-speed railway vehicles requires deep understanding of the behavior of wheels and wheelsets as rotors and wave propagation phenomena in wheel rims, responsible for noise being emitted, corrugation, wheel poligonalization, and wear of a wheel–rail system. The contact problems of wheel–rail interaction in majority of investigations are limited to the dynamic effects caused by the vertical motion of the contact points under assumption that the contact stiffness is linearly dependent on the load. The speed of the contact point is assumed to be constant and equal to the velocity of the rail vehicle motion. In the real systems, many simplifications are not acceptable, that is why further investigations are necessary. In the present paper, some of the results of previous studies are overviewed that are essential for the understanding of the basic phenomena of vehicle–truck interaction from the point of view of the rotor dynamics.

The first part of the paper aims at generalization of the study undertaken by Mahrenholtz [1] to the larger spectrum of rim parameters and wheel dynamics. The second part is devoted to traveling waves' analysis with attention paid to qualitatively different solutions in different regions of Ω, V plane. The other parts of the paper are devoted to influence of residual stress on configuration of this regions, wheels dynamics, and wheelset stability.

R. Bogacz
Department of Civil Engineering, Cracow University of Technology, Kraków, Poland
E-mail: rbogacz@ippt.gov.pl

R. Bogacz · W. Kurnik (✉)
Faculty of Automotive and Construction Machinery Engineering, Warsaw University of Technology, Warsaw, Poland
E-mail: wku@simr.pw.edu.pl

2 Effect of curvature of wheel rim modeled as a beam on elastic foundation

Consider a railway wheel with the wheel–tire modeled as a simple Bernoulli–Euler beam and the wheel plate treated as Winkler's elastic foundation as shown in Fig. 1. The wheel rim height is assumed to be small in comparison with the wheel radius, and the wheel rim cross section is symmetric.

The static normal (circumferential) force in the wheel rim as a curved beam can be described by the equation (see Mahrenholz [1]):

$$\frac{\mathrm{d}^6 N}{\mathrm{d}s^6} + \frac{1}{R^2}\frac{\mathrm{d}^4 N}{\mathrm{d}s^4} + \lambda^4 \frac{\mathrm{d}^2 N}{\mathrm{d}s^2} = 0 \tag{2.1}$$

where the notations are as follows: N—normal force, s—arc coordinate ($s = R\varphi$), c—elastic Winkler's foundation coefficient, $\lambda^4 = c/EI$, R and EI—rim radius and bending stiffness, respectively, and E—Young's modulus.

The solution of Eq. (2.1) has the following form:

$$N(s) = C \exp(rs) \tag{2.2}$$

The solutions of the characteristic equation are as follows:

$$r_{1,...,4} = \pm\sqrt{-\frac{1}{2R^2}\left(1 \pm i\sqrt{\lambda R\sqrt{2} - 1}\right)} \quad (\lambda R\sqrt{2} > 1) \tag{2.3}$$

or in rearranged explicitly complex form

$$r_{1,...,4} = \pm(\delta \pm i)/L \tag{2.4}$$

with $\delta[1/m]$ and $L[m]$ defined by transformation of (2.3) into (2.4).

The solution of Eq. (2.1) can be expressed as follows:

$$N(s) = \exp\left(\frac{\delta}{L}s\right)\left[N_1 \cos\left(\frac{s}{L}\right) + N_2 \sin\left(\frac{s}{L}\right)\right] + \exp\left(-\frac{\delta}{L}s\right)\left[N_3 \cos\left(\frac{s}{L}\right) + N_4 \sin\left(\frac{s}{L}\right)\right] \tag{2.5}$$

where $N_{1,2,3,4}$ are constants to be calculated from the boundary conditions for the radial displacement w:

$$w'(s = 0) = 0, \quad w'(s = \pi R) = 0, \quad -EIw'''(s = 0) = \frac{F}{2}, \quad w'''(s = \pi R) = 0 \tag{2.6}$$

where F is the external contact force, as shown in Fig. 1.

Under assumption that the normal force is constant (N_0), the curved beam equation has the following form:

$$\frac{\mathrm{d}^5 w}{\mathrm{d}s^5} + \left(\frac{1}{R^2} - \frac{N_0}{EI}\right)\frac{\mathrm{d}^3 w}{\mathrm{d}s^3} + \frac{c}{EI}\frac{\mathrm{d}w}{\mathrm{d}s} = 0 \tag{2.7}$$

It is enough to neglect the first term in the brackets to obtain the equation for a straight beam subjected to longitudinal force N_0.
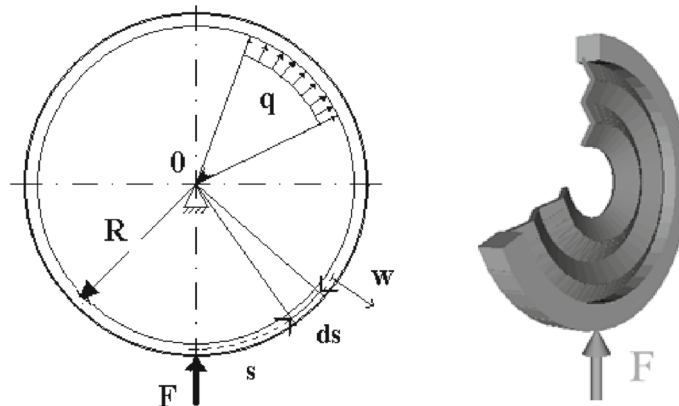

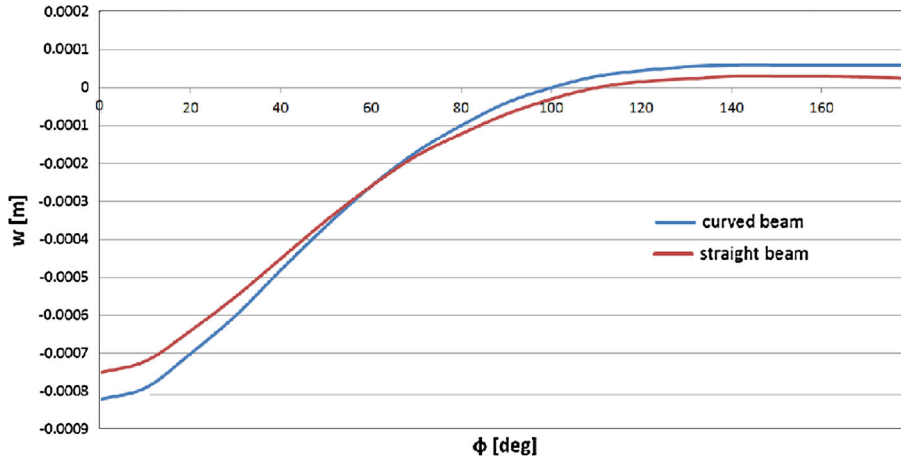
Fig. 1 Railway wheel rim model

Fig. 2 Comparison of displacements $w(\Phi)$ for straight and curved beams for $c = c_1 = 2.26 \times 10^8$ N/m^2
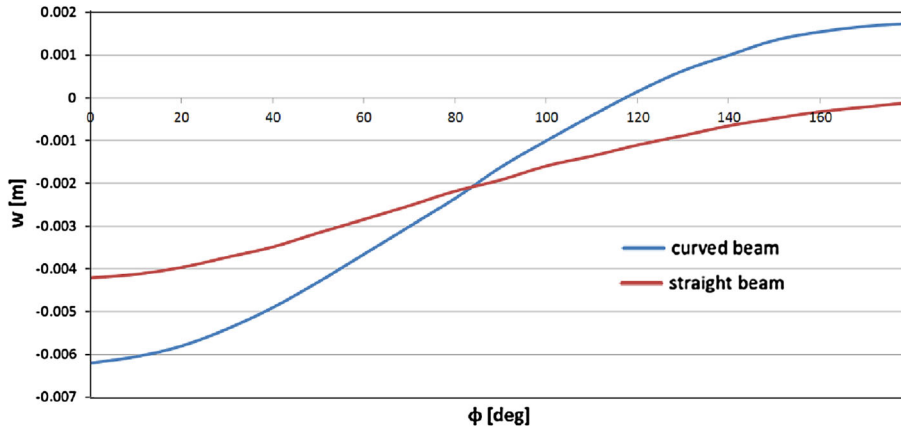

Fig. 3 Comparison of displacements $w(\Phi)$ for straight and curved beams for $c = c_2 = 2.26 \times 10^7$ N/m^2

To generalize the results obtained in Ref. [1] and show that the results of deformation strongly depend on wheel plate stiffness parameter c and the normal force N_0, we consider some examples for the following parameter values:

$E = 2.1 \times 10^{11}$ N/m^2, $I = 3.93 \times 10^{-6}$ m^4, $A = 9.26 \times 10^{-3}$ m^2, $R = 0.4325$ m, $F = 1.2 \times 10^5$ N, and three values of Winkler's foundation stiffness: $c_1 = 2.26 \times 10^6$ N/m^2, $c_2 = 10^{-1} \times c_1$ and $c_3 = 10^{-2} \times c_1$. The results are shown in Figs. 2, 3, and 4, where the displacements of the rim are compared for two models—straight and curved Euler beam.

One can see that lowering wheel plate stiffness, e.g., by placing rubber interconnection between rim and wheel plate to reduce vibration has to be undertaken together with the assumption that the rim must be modeled as a curved beam.

3 Phase velocity of wave propagated in the rim

After including inertia term into Eq. (2.1) with ρ denoting rim mass density and the following notations:

$$W(s, t) = w(s, t) - w_0, \quad a^2 = \frac{EI}{\rho A}, \quad k_s = \frac{1}{R}, \quad c_0 = \frac{c}{\rho A}, \quad T = \frac{N}{A}, \tag{3.1}$$

we obtain the equation of the wheel rim radial motion in the form:

$$\frac{\partial^2 W}{\partial t^2} + a^2 \frac{\partial^4 W}{\partial s^4} + \left(a^2 k_s^2 - T\right) \frac{\partial^2 W}{\partial s^2} + c_0 W = 0. \tag{3.2}$$
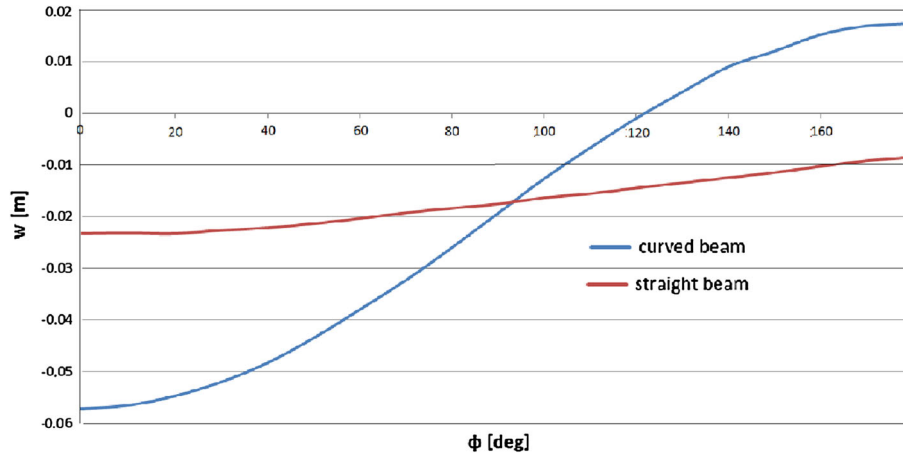
Fig. 4 Comparison of displacements $w(\Phi)$ for straight and curved beam for $c = c_3 = 2.26 \times 10^6 \text{ N/m}^2$
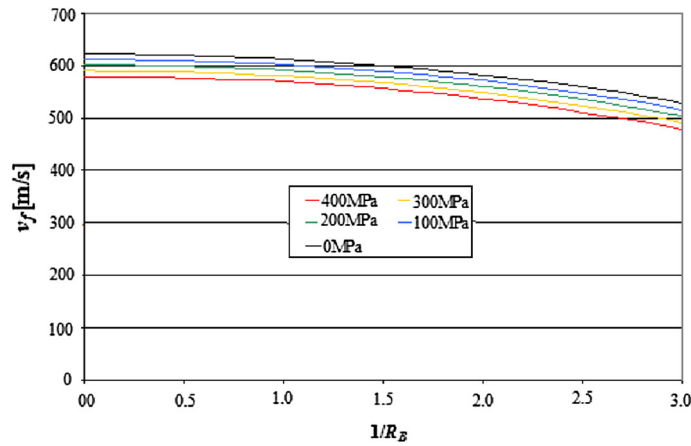

Fig. 5 Influence of rim curvature $(1/R_B)$ on the phase velocity, v_f for $c = 2.26 \times 10^8 \text{ N/m}^2$

Now, we are looking for solution of Eq. (3.2) in the form of a traveling wave:

$$W(s, t) = B \sin k(s - v_f t), \tag{3.3}$$

where k and v_f denote wave number and phase velocity, respectively. The phase velocity can be expressed as:

$$v_f = \pm \frac{\sqrt{a^2 k^4 + k^2 \left(T - a^2 k_s^2\right) + c_0}}{k} \tag{3.4}$$

Relation (3.4) between the phase velocity and the wave number for exemplary parameter values $E = 2.1 \times 10^{11} \text{ N/m}^2$, $A = 9.26 \times 10^{-3} \text{ m}^2$, $\rho = 7{,}800 \text{ Ns}^2/\text{m}^4$ are presented in Figs. 5 and 6, like in Ref. [2].

The above results allow one to evaluate the influence of the beam curvature and residual stress on the phase velocity and its critical value in the wheel–tire. These results comprise a first step to determine traveling waves generated by a moving and oscillating force and a next step for investigating stability of wheelset–track and train–track interaction. The oscillatory load results from periodical wheel structure, periodicity of sleeper spacing, and corrugations.

The equation of motion of the Bernoulli–Euler beam subjected to moving oscillating force can be described as follows:

$$EI \frac{\partial^4 W}{\partial s^4} + \rho A \frac{\partial^2 W}{\partial t^2} + \left(\frac{EI}{R^2} - T\right) \frac{\partial^2 W}{\partial s^2} + \eta \frac{\partial W}{\partial t} + cW = F_0 \delta \left(s - vt\right) \cos \omega t \tag{3.5}$$
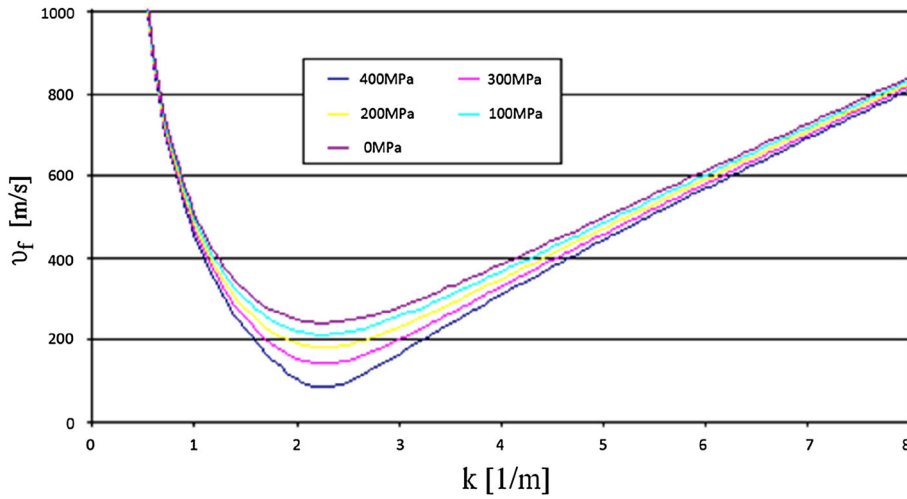
Fig. 6 Phase velocity vs. wave number for various residual stress and for wheel plate elastic coefficient $c = 2.26 \times 10^7$ N/m^2
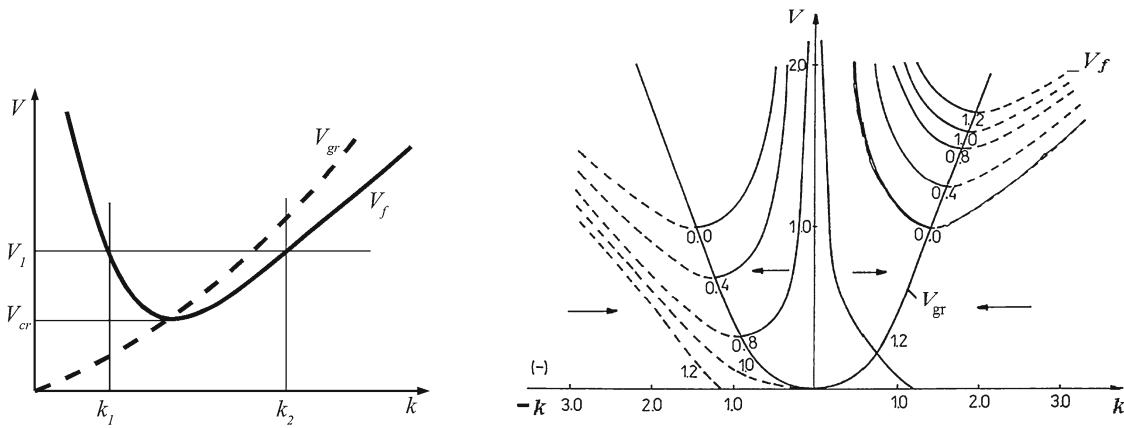

Fig. 7 Phase and group velocity versus wave number, k and directions of wave propagation for various frequencies of excitation, $\Omega = (0–1.2)$

After transformation of Eq. (3.5) to a moving coordinate system connected with the contact force and introducing dimensionless variables, we obtain the equation of motion in the form:

$$\frac{\partial^4 W_r}{\partial X^4} + 4\frac{\partial^2 W_r}{\partial \tau^2} - 8V\frac{\partial^2 W_r}{\partial X \partial \tau} + 4V^2\frac{\partial^2 W_r}{\partial X^2} + \left(4V^2 + \frac{4}{R_B^2} - 4N_B\right)\frac{\partial^2 W_r}{\partial X^2} + 4W_r = 8\delta(X)\cos\Omega\tau, \quad (3.6)$$

where R_B and N_B are dimensionless radius of the rim and dimensionless residual stress resultant, respectively, and

$$W_r = W\frac{8EIa_0^3}{F_0}, \quad \Omega = \omega\sqrt{\frac{\rho A}{c}}, \quad V = v\sqrt[4]{\frac{(\rho A)^2}{4cEI}}, \quad a_0 = \sqrt[4]{\frac{c}{4EI}}, \quad X = (s - vt)a_0, \quad \tau = t\sqrt{\frac{c}{\rho A}}.$$

To determine the proper solution of the problem formulated in Ref. [3], one has to find solution in the form of a traveling wave that satisfies the Sommerfeld condition of radiation [4], taking into account that energy is transported with the group velocity.

As shown in the graph on the left-hand side of Fig. 7, for a given value of speed V_1 and for positive values of wave number k_1, the group velocity, V_{gr}, is smaller than the phase velocity, V_f—that is why this wave
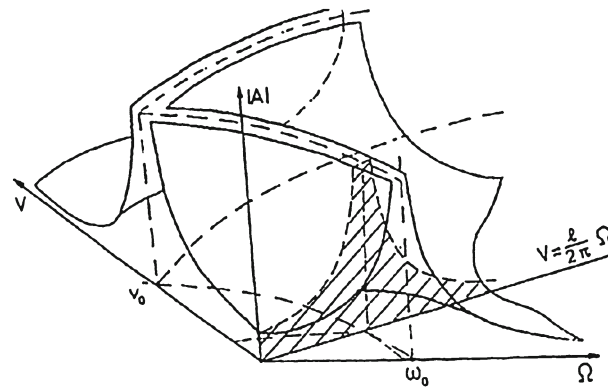
Fig. 8 Amplitude of displacement as function of speed V and frequency Ω. An exemplary resonance curve as cross section of the spatial graph $V = \Omega l/2\pi$ is visible
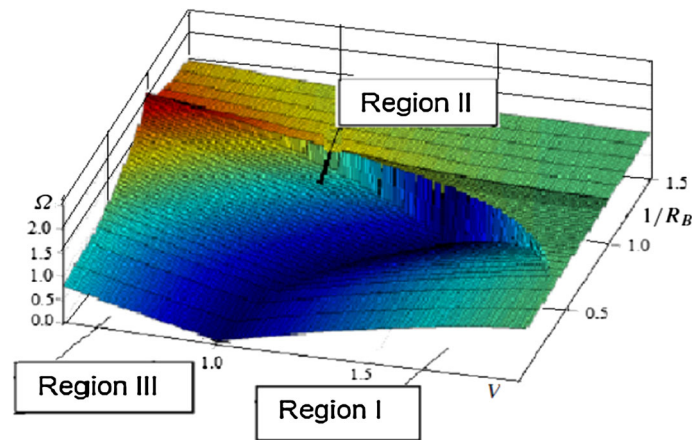

Fig. 9 Regions of qualitatively different solution as function of the velocity V, excitation frequency Ω and curvature $(1/R_B)$ with the residual stress $N_B = 0$

should propagate from the source of excitation. The wave with wave number k_2 can propagate to the source of excitation because value of group velocity is greater than that of phase velocity.

In the case of straight Bernoulli–Euler beam, the dependence of displacement on velocity of force motion V oscillating with frequency Ω is shown in Fig. 8. The resonance curves divide the speed–frequency plane into the three regions of qualitatively different solutions.

It can be seen in Fig. 9 that large values of wheel–tire curvature $(1/R_B)$ considerably influence the configuration of the three regions with qualitatively different solutions.

The influence of the residual stress is more important because compressive stresses reduce the critical wave velocity. This effect is shown in Fig. 10.

The visualization of the qualitative difference of the solutions in the first and second regions is shown in Fig. 11.

The tire of the wheel can be modeled in a more complicated way, i.e., as the Rayleigh beam or the Timoshenko beam, as the rail can be modeled. A very complicated wheel model was investigated in Ref. [5], where the curved beam could exhibit radial and circumferential displacements as well as lateral ones as a result of out-of-plane bending and torsion. The wheel plate was modeled by an elastic Winkler foundation. The crucial result of that investigation is connected with a very high resonance of the wheel rim at the vehicle speed of about 200 km/h in the case when the wheel is excited in the contact area by a force or a spin moment. An example is shown in Fig. 12. It can be seen that for the speed greater than zero, each eigenfrequency is divided into two values, corresponding to the waves traveling in the direction of the rolling motion and to the
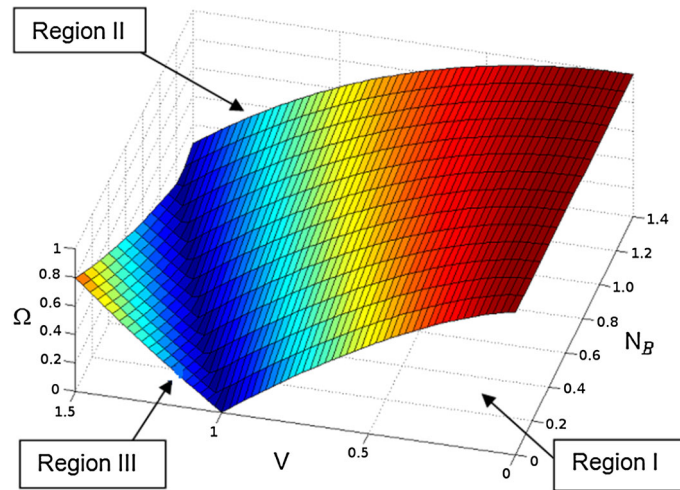
Fig. 10 Regions of solutions depending on velocity V, excitation frequency Ω, and residual normal force N_B for straight beam $(1/R_B = 0)$
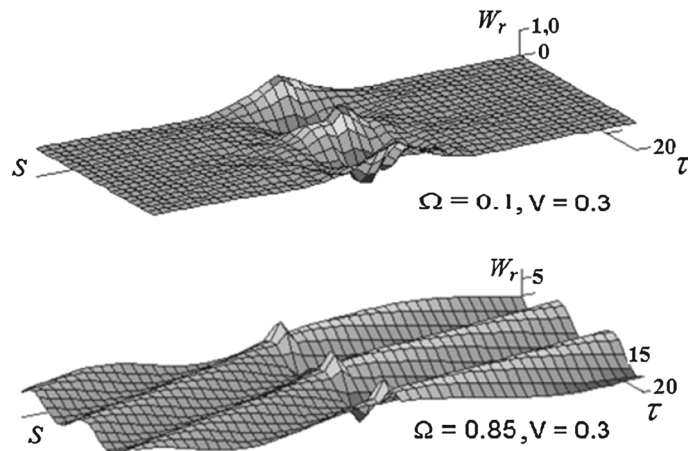

Fig. 11 The traveling wave solution in the first and second regions of the speed–frequency plane

waves moving in the opposite direction. The waves with increasing frequency are much more amplified than the other ones.

The description of such a complicated model is made by four partial differential equations, and the solution is obtained in the form of traveling wave. More details can be found in Ref. [5]. The solution of wheel dynamics makes possible an investigation of motion of a wheelset as a flexible system. For such an analysis, in case of rigid axle one will need 14 coupled differential equations for the wheels and the wheelset.

Using the fixture of symmetry (**S**) and anti-symmetry (**A**) and assuming constant speed along the track, it is possible to reduce the number of equations to nine. Solving the set of equations, we obtain trajectories of wheelset motion with positions of the wheelset axles as shown in Fig. 13. In Ref. [5], top and front views of a wheelset are presented.

The four situations shown in Fig. 13 correspond to the following motions:

- **S–S**—wheels vibrate in-phase, symmetrically with respect to the wheelset center, the wheelset center moves vibrating sinusoidally in the vertical direction. The trajectory seen from the top is a straight line, and the axle is perpendicular to the track.
- **S–A**—wheels vibrate in-phase, anti-symmetrically with respect to the wheelset center, the wheelset center moves vibrating sinusoidally in the horizontal direction and the axle is perpendicular to the track, as in the **S–S** case.
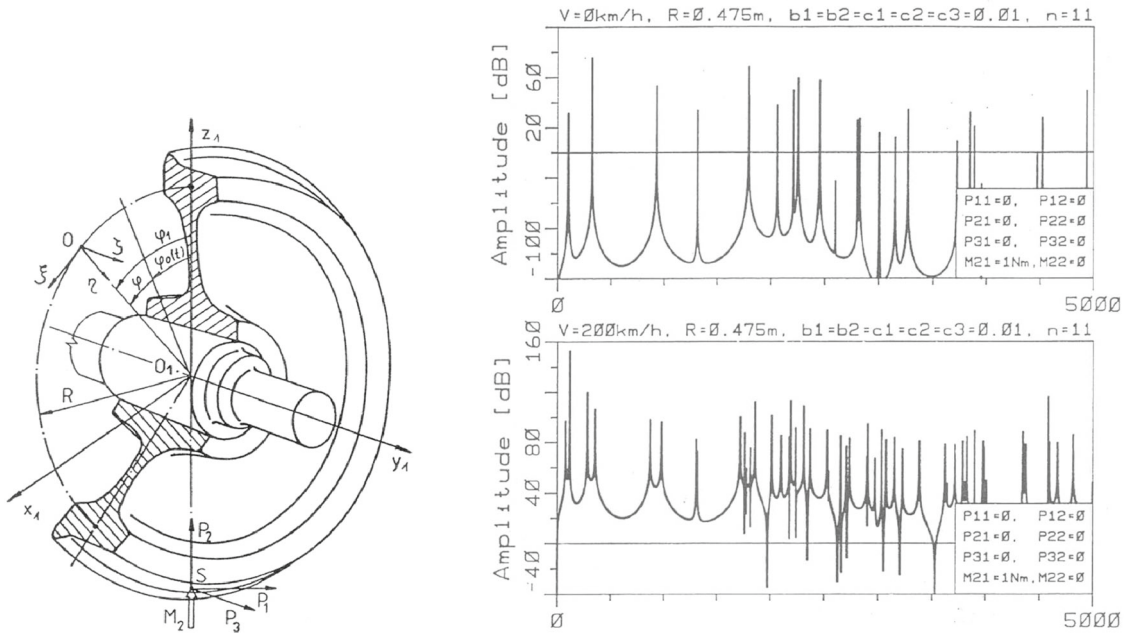
Fig. 12 Three-dimensional wheel model and flexural radial displacements at the speeds $V = 0$ and $V = 200$ km/h
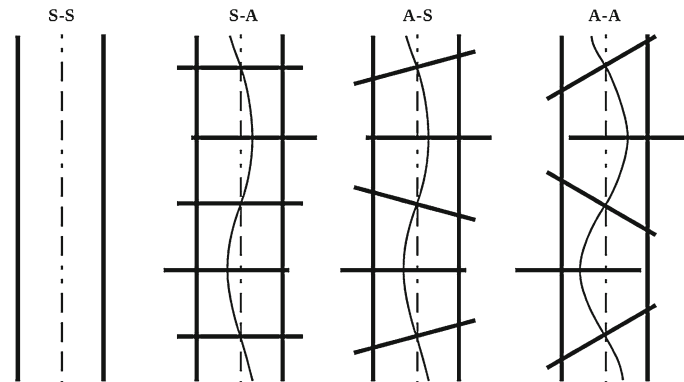

Fig. 13 Trajectories of wheelset center and positions of axles in chosen points of motion

- **A–S**—wheels vibrate out-of-phase, symmetrically with respect to the wheelset center, the wheelset center moves vibrating sinusoidally in the horizontal direction and the axle rotates with an oscillating inclination with respect to its initial position.
- **A–A**—wheels vibrate out-of-phase, anti-symmetrically with respect to the wheelset center, the wheelset center moves vibrating sinusoidally in the horizontal direction and axle rotates horizontally and vertically with oscillating inclination with respect to the position perpendicular to the track. Details of various wheels eighenmodes are given in Ref. [6]. Two exemplary modes of wheelset according to Ref. [7] are shown in Fig. 14.

One can notice that in the case of anti-symmetric modes lateral forces are acting on the rail what needs further analysis (which does not belong to rotor-dynamical problems). In the case of modern light railway vehicles with independent drive systems the above mentioned instability phenomena do not appear, but the dynamic electromechanical coupling occurs [8].
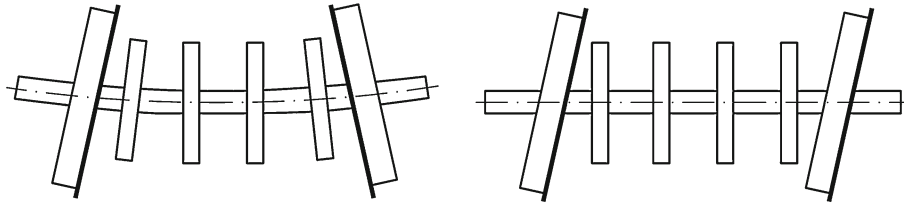
Fig. 14 Symmetric (*left*) and anti-symmetric (*right*) modes of wheelset vibration
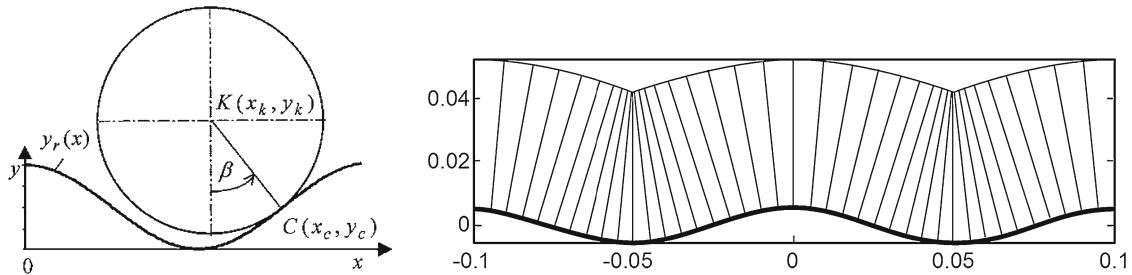

Fig. 15 Corrugated rail and trajectory of wheel center motion

4 Remark on wheel–rail contact with corrugation

Another very important dynamical effect is related to corrugated or poligonalized wheel motion on straight or wavy rail. Majority of investigations were conducted assuming that the wheel radius is small in comparison with the radius of the rail roughness. A study addressing this problem is devoted to the change of velocity of the load motion (horizontal) and the acceleration of the wheel center in the vertical direction.

The position of the contact point and the wheel center and the trajectory of the wheel center in case of sinusoidal corrugation are shown in Fig. 15 left and right, respectively. It is interesting that in the ideal case of stiff contact and wheel curvature approaching curvature of corrugation, the acceleration tends to infinity. The elastic wheel–rail contact limited such picks of acceleration, but introduces resonance phenomena connected with the contact stiffness. A detailed discussion on this topic can be found in Ref. [9]. Some results of wavelets application one can find in Ref. [10].

5 Concluding remarks

The results presented in this paper demonstrate the importance of rotor-dynamical effects in high-speed train wheel–track interaction. Some of the considered effects are related to the fundamental phenomena of train–track dynamics in general, like traveling wave solution with regard to the group velocity of waves and particularly the wheel–rail and wheel–set–track interaction. The wheel–rail interaction is influenced by the load which causes deformations of the wheel plate and the wheel rim, what in turn changes the contact point position. This problem is discussed in Ref. [11].

References

1. Mahrenholtz, O.: Elastic beam-like ring on Winkler foundation. In: Katsikadelis, J.T., Beskos, D.E., Gdoutos, E.E. (eds.) Advances in Applied Mechanics, pp. 214–219. Honorary Volume for Professor A.N. Kounadis, Athens (2000)
2. Bogacz, R., Kocjan, M., Kurnik, W.: Dynamics of wheel–tyre subjected to moving oscillating force. Mach. Dyn. Probl. **27**(4), 168–179 (2003)
3. Mathews, P.M.: Vibration of beam on elastic foundation. Z. Angew. Math. U. Mech. **38**, 105–115 (1958)

4. Bogacz, R., Krzyżyński, T., Popp, K.: Application of Floquet's theorem to high-speed train/track dynamics. In: DSC-vol.56/DE/vol.86, Advance Automotive Technologies, ASME Congress, pp. 55–61 (1995)
5. Bogacz, R., Dżuła, S.: Dynamics and stability of wheelset–track interaction modeled as nonlinear continuous system. Mach. Dyn. Probl. **20**, 23–34 (1998)
6. Noga, S., Bogacz, R.: Algorithm to identify the mode shapes of the circular or annular systems with the discontinuous features. In: Łodygowski, T. et al. (eds.) CMM-2013—Computer Methods in Mechanics, pp. MSo7-5–o7-6. Poznań (2013)
7. Bogacz, R., Meinke, P., Dżuła, S.: Vehicle/track-dynamic interaction for high speed-frequency range. In: Bogacz, R., Popp, K. (eds.) Dynamical Problems in Mechanical Systems, pp. 165–179. IPPT PAN, Warsaw (1993)
8. Szolc, T., Konowrocki, R., Michajłow, M., Pregowska, A.: An investigation of the dynamic electromechanical coupling effects in machine drive systems driven by asynchronous motors. Mech. Syst. Signal Process. **49**, 118–134 (2014)
9. Bogacz, R., Frischmuth, K.: On some new aspects of contact dynamics with application in railway engineering. J. Theor. Appl. Mech. **50**(1), 119–130 (2012)
10. Bogacz, R., Krzyżyński, T., Kozioł, P.: An analysis of the dynamic effects of periodic structures subject to a moving load. In: Pombo, J. (ed.) Proceedings of the Railways 2012 Conference, Las Palmas de Gran Canaria 116, 14 pp (2012)
11. Bogacz, R., Konowrocki, R.: On the new effects of wheel–rail interaction. Arch. Appl. Mech. **82**, 1013–1023 (2012)